Journal of Engineering and Applied Sciences 3 (11): 872-883, 2008
ISSN: 1816-949X

The Calculation of Ball Bearing Nonlinear Stiffness Theoretical and Experimental Study with Comparisons

[1]Dougdag Mourad, [2]N.E. Titouche, [3]M. Djaoui and [4]Ouali Mohammed
[1]Chargé de Recherche, [2]Attaché de Recherche,
[3]Ingénieur de Laboratoire Niveau III,
CRNB B.P. 180 Ain-Oussera, 17200, Willaya de Djelfa, Algérie
[4]Département de Mécanique, Faculté des Sciences Pour l'Ingénieur,
Université Saad Dahlab Blida, B.P. 27, Route de Soumâa, Blida, Algérie

Abstract: This study presents a theoretical and an experimental nonlinear stiffness ball bearing study in static and dynamic mode. The theoretical study allows us to build an analytical model where the construction is based on different approaches from the traditional ones. Firstly, the developed model is based on other forms to determine ball's deformation. Secondly, it describes the nonlinear dynamic behaviour of the ball bearings by considering the balls scrolling in the cage and the effect of rotating vector load. These modifications were done hoping to ameliorate ball bearings stiffness computing and having positives impacts on design and maintenance domain of rotating machines. To verify experimentally the developed model, in static and dynamic conditions, some numbers of compression tests were done on the ball bearings, in sight to measuring experimentally the rigidity. This requires the mooring system adaptation of a mechanical universal testing machine to receive the ball bearing specimen. Experimental results where obtained under imposed load mode, analysed and confronted to the theoretical model ones. Finally, it was also a proceeding to the confrontation of the obtained results to those of the known models.

Key words: Modelling, ball bearings, stiffness, experience, mechanical testing, balls scrolling, design, maintenance

INTRODUCTION

In this research, we are interested to the theoretical and experimental ball bearings study. The mechanical behaviours modelling of this device part is mainly based on the stiffness calculation which is obtained by the determination of the local (Bourgain *et al*., 1988; Shigley and Mitchel, 1983) and global (Timoshenko, 1968) ball bearing deformations under loadings.

Ball bearing took importance since Palmgren (1959), Harris (1996) and Eschmann *et al*. (1985) research. The purpose was to describe the vibrations transfer towards the structure. In fact, the ball bearings introduce several sources of nonlinearities associated with the mechanical gaps and the hertzians contacts between the rolling balls and balls races.

Hertz contacts theory allows Palmgren (1959) to establish analytical models behaviour of axial and/or radial load ball bearing from a "force-displacement" viewpoint. The principal Palmgren approach interest is to consider the radial and axial deflections between the two ball bearing rings (Estocq, 2004).

It is to note that calculations are done around an equilibrium position corresponding to the ball bearing static loading. Therefore, the stiffness is evaluated by static or quasi-static analysis. The stiffness, usually, is confused as an isotropic springs. It is the model with concentrated parameters. But this approach does not consider the coupling binding-tensile. Rajab (1982) introduced the coupling and Young (1988) included the axial load effect.

Recently, other models more adapted to the formalism "finites elements" were developed. Lim and Chin (1989) has proposed matrix model of 5×5 and he used the Kraus *et al*. (1987) experimental results to validate his model. De Mull *et al*. (1989) proposed an approach similar

Corresponding Author: Dougdag Mourad, Chargé de Recherche, COMENA/CRNB/DTN/Laboratoire des Etudes Mécaniques, CRNB B.P. 180 Ain-Oussera, 17200, Willaya de Djelfa, Algérie

to that of Lim but based on a vectorial description and matrix formalism. Bourdon and Adelin (1997) has based on the De Mul model, with considering a possible ring's swinging angle. Fukata *et al.* (1985) proposed a model which it considers the balls inertia.

The dynamic stiffness calculation is usually obtained by analytical calculation without experimental check Beatty and Rowan (1982). Marsh and Yantek (1997) and Bogard *et al.* (2002) showed that the analytical model presents difficulties and gives bad answers to the dynamic calculation requirements. Therefore, they adopted experimental methods to measure dynamic stiffness.

The contribution in this research consists to suggest a different approach from existing works to obtain a ball bearing static and dynamic stiffness model; in fact, the majority of preceding work (Palmgren, 1959; Harris, 1996; Eschmann *et al.*, 1985; Lim *et al.*, 1989; De Mul *et al.*, 1989; Bourdon and Adelin, 1997; Fukata and Chin, 1985) or those of Yakhou (1999), Campedelli (2002), Estocq (2004), Dehez (2004), Hentati and Col (2005), Yuzhong (2006) and Krämer (1993) are based on the Hertz theory (Bourgain *et al.*, 1988; Shigley and Mitchel, 1983; Louf, 2003; Lelkes, 2002) for the balls deformations calculation, but in our study, we introduced a different approach to calculate deformations. Moreover, we have experimentally checked the static and the dynamic stiffness model and compared our model results to some existing models.

THEORETICAL MODEL

Several bearing types are used in the revolving machines. Due to their complexity and their diversity; we are interested only in the ball bearing cases (Fig. 1).

The theoretical development of this model requires a kinematics modelling, a contact mechanism, an equivalent model loading and coupling considerations.

The concepts concerning the geometrical characteristics and physics and the kinematics study are largely commented on Shigley and Mitchel (1983), Moret (1995) and Chevalier (1979).

Stiffness computing: The stiffness evaluation is based on Rajab (1982) model. Thus, we calculate deformations and corresponding loads to deduce the stiffness into quasi-static mode (Fig. 2).

The ball bearing total deformation is composed of the local deformation due to the ball contact with the higher and lower housing ring areas and to the balls global elastic compression.

Due to the significant size of various ball bearing stiffness analytical calculations; we are limited, in this study, only on radial stiffness computation.

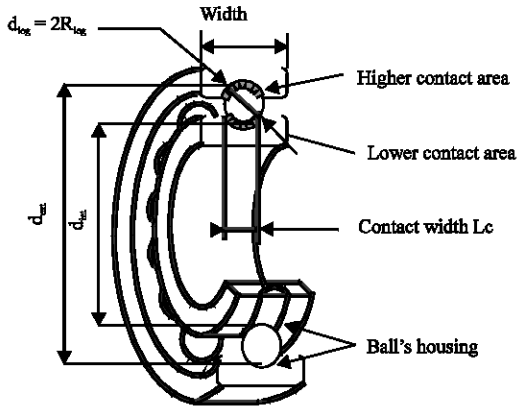

Fig. 1: Ball bearing section representation

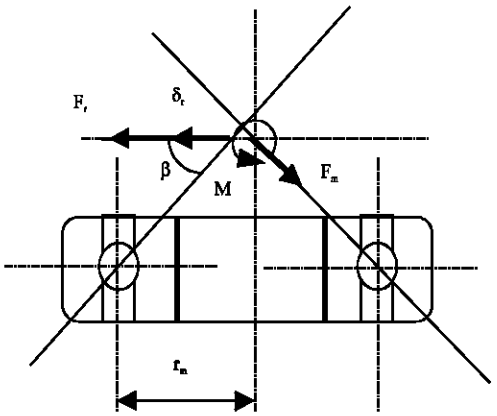

Fig. 2: Diagram of maximum force applied to the ball bearing

To obtain this stiffness, we calculate: the local deformation resulting from the contact between the ball and ring according to the Hertz law (Bourgain *et al.*, 1988; Shigley and Mitchel, 1983)

- The elastic ball deformation according to the elasticity law (Timoshenko, 1968)
- The loads which generated these deformations
- The stiffness by using the Rajab (1982) technique

Hypothesis: The considered hypotheses are:

- We suppose that we have the same locals or hertzians deformations on the 2 sides of the ball and on the 2 rings
- We don't take into account:
  - The lubrication (the hydrodynamic effects are neglected)
  - The frictions

  - The interactions due to the balls train (cage)
  - The 2 rings elastic deformations
- We suppose that we have the same distance between balls in the cage
- We consider a no oblique bearing contact ($\beta = 0$)
- We consider the bearing with clearance
- We suppose that depth (h_r) due to the Hertzian contact is small, stay constant for corresponding force and it is slightly influenced by the ball's elastic deformation
- The loading distributed used for the equivalent force calculation on a ball is taken before the contact of the shaft with ball bearing like a simplifying approach
- Initially, the revolving vector loading is supposed at the position of $\phi = -\pi/2$

Calculation procedure: Bearing total deformation is composed of global balls elastic compression Fig. 3b and local deformation according to the Hertz law (Louf, 2003; Lelkes, 2002) due to the ball contact with the higher and lower housing ring areas Fig. 3a.

Calculation is done as follows: according to the Hertz law (Bourgain *et al*., 1988; Shigley and Mitchel, 1983), local deformation of one side is given by h_r for a contact between ball and ring:

$$h_r = R - \sqrt{R^2 - a^2} \quad (1)$$

With:

$$a = \sqrt[3]{\frac{3F}{8}\frac{[(1-\nu_1^2)/E_1]+[(1-\nu_2^2)/E_2]}{(1/d_1)\pm(1/d_2)}} \quad (1^*)$$

We look for resemblance between Eq. (1) and those found in literature as follow.

According to Louf (2003), Lelkes (2002), Bourgain *et al.* (1988) and Shigley and Mitchel (1983), the Hertz law gives the deformation (Fig. 3a) under the following form:

$$\delta = \frac{\pi.a.p_0}{2E^*}$$

With:

$$\frac{1}{E^*} = \frac{1-\nu_1^2}{E_1} + \frac{1-\nu_2^2}{E_2} \text{ and } p_0 = \frac{3.F}{2.\pi a^2} \text{ (Shigley, 1983)}$$

If we reformulate (δ) by using (a) according to Eq. (1)*, we find the form (2) as in (Palmgren, 1959; Lim and Chin, 1989; De Mul *et al*., 1989 and Bourdon and Adelin, 1997):

$$F = K\,\delta_h^{3/2} \quad (2)$$

where:

K = A stiffness factor

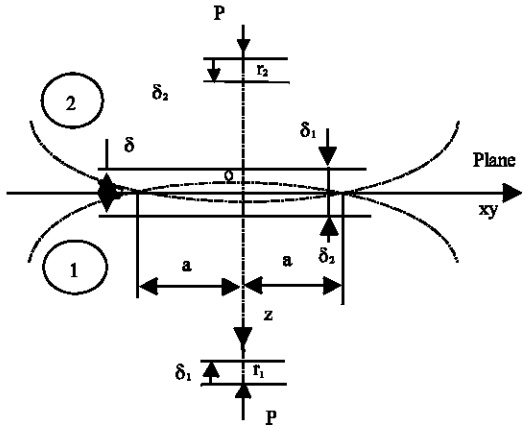

Fig. 3a: Local deformation according to Hertz law (Louf, 2003; Lelkes, 2002)

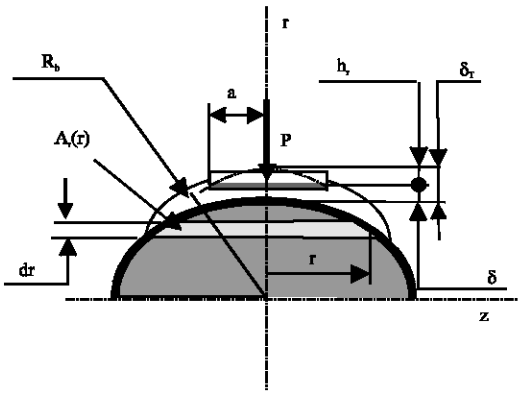

Fig. 3b: Local and global elastic deformation of a symmetric part of ball for our deformation model

The 2 Eq. (1 and 2) have the similar bases (Hertz law) but, in our method, local deformation h_r was obtained geometrically and directly from contact shape. This allows a new approach to calculate step by step deformations.

- Using Timoshenko (1968) beam, according to Hook Law, allows modelling the ball compression behaviours under the resulting load (F), knowing that the ball suffer a local deformation (h_r) with a width of (a). This gives elastic global radial deformation (δr) equation:

$$\frac{d\delta}{dr} = \frac{F}{EA(r)} \quad (3)$$

- Resolution of this equation in symmetrical domain of r(0..(R-h_r)) Fig. 3b gives global deformation which we add total one for two sides as:

$$\delta_T = 2.(\frac{F}{\pi E d_b}\ln\left[\frac{d_b}{h_r}-1\right]+2.h_r) \quad (4)$$

Equation (4) includes the elastic compression of both sides of ball, supposed similar and the same thing on both rings (Fig. 3a).

Equation (4) permit adopting a method to construct the curve of force-displacement $f(\delta_T)$. We have for each applied force F_i a corresponding local deformation $(h_r^{(i)})$ using Eq. (1). We, then introduce $(h_r^{(i)})$ in Eq. (4) to obtain the corresponding total deformation $\delta_T^{(i)}$.

The distributed loading on ball bearing is illustrated in Fig. 4. For a distributed loading slice on one ball between $(\varphi_i\ \varphi_{i+1})$ (Fig. 5), we have the following form:

$$q(\varphi) = q_0\sqrt{1-\cos^2(\varphi)} = q_0.\sin\varphi$$

The total loading F_i applied to i^{2nd} ball is:

$$F_i = Lc\int_{z_i}^{z_{i+1}} q(z)dz = LcRq_0\int_{\varphi_i-\frac{\varphi_n}{2}}^{\varphi_i+\frac{\varphi_n}{2}} -\sin^2\varphi d\varphi \quad (5)$$

After the resolution of Eq. 5 for $\varphi_n = 2\pi/n$ and $q_0 = 2F/RL_c\pi$ we obtain:

$$F_i = \frac{F}{2\pi}\left[\sin 2(\varphi_i+\pi/n)-\sin 2(\varphi_i-\pi/n)-4\pi/n\right] \quad (6)$$

The radial load is defined by:

$$F_{ri} = |F_i|\ \sin\varphi_m^{(i)} \quad (7)$$

with

$$\varphi_m^{(i)} = (\varphi_i+\varphi_{i+1})/2$$

The law linking loads to deformations Rajab (1982) is expressed as follows:

$$K_{rr}^{(b)} = dF_r/d\delta_T \quad (8)$$

Using Eq. (4), we obtain the (force-displacement) curve $f(\delta_T)$. With Eq. (8), we obtain the ball stiffness for the nominal loading on each ball expressed by:

$$k_{rr}^{(b)} = \frac{F_r}{2\frac{F_r}{\pi E d_b}\ln\left[\frac{d_b}{h_r}-1\right]+4.h_r} \quad (9)$$

To obtain the total ball bearing radial stiffness, we consider all loaded balls Fig. 5 which are not uniformly loaded and their positioning in cage is changing due to the ball bearing kinematics, consequently, stiffness is varying. The stiffness becomes dependent on balls position, as a raison considering the balls level loading and the balls scrolling (positioning).

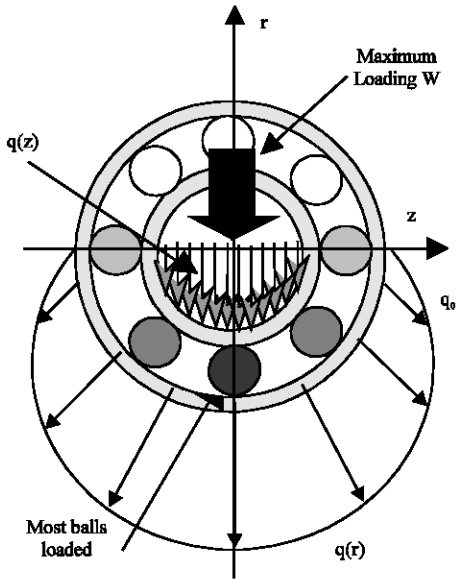

Fig. 4: Loads distribution model on ball bearing before contact q(z) and after contact q(r)

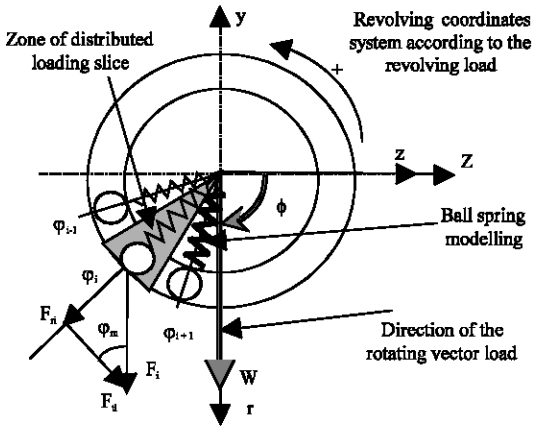

Fig. 5: Balls radial loading model, resulting forces

Level load and balls scrolling: Figure 6 illustrates the level of load applied on each ball. The ball bearing has approximately half of balls gradually loaded and the others are free loading.

Figure 7 represents the principal balls positioning states for one cycle. The scrolling of balls in cage causes the stiffness change in a nonlinear form.

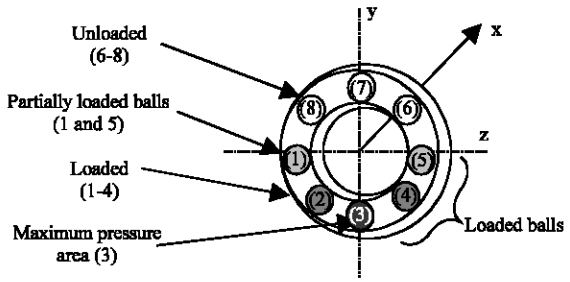

Fig. 6: Level load applied on balls

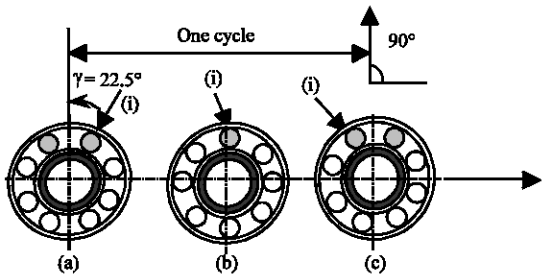

Fig. 7: Balls scrolling in cage (positioning)

In order to consider the balls level loading, load mode (Fig. 4), balls scrolling and revolving vector load, we propose the following form:

$$K_{rr}(\gamma)=\sum_{i=1}^{m}\left|K_{rr}^{(bi)}.\cos(\gamma_i-\phi)\right| \quad (10)$$

With:

γ_i = The $(i)^{2nd}$ ball angular position

$$\gamma_i=\gamma_{i-1}+\varphi_n$$

where:

φ_n = $2\pi/n$

$K_{rr}^{(bi)}$ = Ball stiffness considered

γ_i = The first half of bearing and not considered in the other half

$$\gamma = \omega_{ca}.\, t+\gamma_0$$

where:

γ_0 = Initial position of each ball

$$\phi = \omega\, .\, t + \phi_0$$

where:

ϕ_0 = Initial position of revolving loading vector

m = The loaded ball number ($m \approx n/2$)

Equation (10) choice is justified by both ways, one in which the radial forces are expressed according to the Eq. (6 and 7) and the other in which the balls are positioned and loaded into cage. This Eq. (10) can be also identified by function of radial distance between out of place ring and fixed one; that's why the form match with sine function. On the other hand, several authors use a similar form as Estocq (2004) to express the balls deformation according to the angular position.

PALMGREN AND DE KRÄMER MODELS

Palmgren formula-radial and axial stiffness: The results in the following table from Palmgren (1967) research.

Radial load $\delta_a = 0$

Bearings kinds:

Loads on rolling elements

$$Q=\frac{5F_r}{i.Z.\cos\beta}$$

balls

$$\delta_r = 0.0020Q^{\frac{2}{3}}D_w^{-\frac{1}{3}}$$

rollers

$$\delta_r=\frac{0.0006}{\cos\beta}l_a^{-0.8}Q^{0.9}$$

With:

δ_r = Radial displacement

δ_a = Axial displacement

F_r = Radial load

F_a = Axial load

D_w = Elements diameter

l_a = Rollers lengths: elements number

I = Elements row number

Q = Maximal load applied on elements

The deformation is expressed by:

$$\delta_r=\left[10^{-4}\frac{0.0020}{(\cos\beta)^{\frac{2}{3}}}\left(\frac{5}{10}\right)^{\frac{2}{3}}\right]F_r^{\frac{2}{3}}d_b^{-\frac{1}{3}}(i.n)^{-\frac{2}{3}} \quad (11)$$

where, $\beta = 0$.

Krämer formula-radial and lateral: The results from Krämer (1993) work of the ball bearings stiffness k_r is given by:

$$k_r=\frac{nF}{x_r} \quad (12)$$

where, n and x_r are given as follows:

Bearings	n	x_r
balls	3/2	$1.2\times10^{-7}\times d^{-\frac{1}{3}}\times Z^{-\frac{2}{3}}\times F^{\frac{2}{3}}$
rollers	1/0.9	$1.11\times10^{-9}\times l^{-0.8}\times Z^{-0.9}\times F^{0.9}$

With:

x_r = Displacement
d = Balls diameter
l = Rollers lengths
F = Load

EXPERIMENTAL VALIDATION OF MODEL

Device: The universal testing machine of type INSTRON 1185 was used for tests realization on the ball bearings (reference FLT ISKRA 6203Z) with 8 balls. This device is composed of a 100KN capability mechanical frame controlled by an electronic part.

This installation allows imposing a load on a sample specimen between two metals bits at the frame and monitoring speed of applied force using electronic device (Fig. 8).

The frame: The installation frame is constituted of a crosspiece guided and mounted on a 2 screw which transmits a controlled displacement at low and stable speeds.

Mooring system: To hold the ball bearings in their loading position, a mooring system was especially conceived. This system combines 3 distinct parts:

Low cycle fatigue testing bit: This bit has significant dimensions, consequently has significant rigidity. In static, it can test a specimen until 100 KN.

A testing bit COD: This bit is made in special steel (maraging steel), it has a static capability of 100 KN load and 60 KN into dynamic.

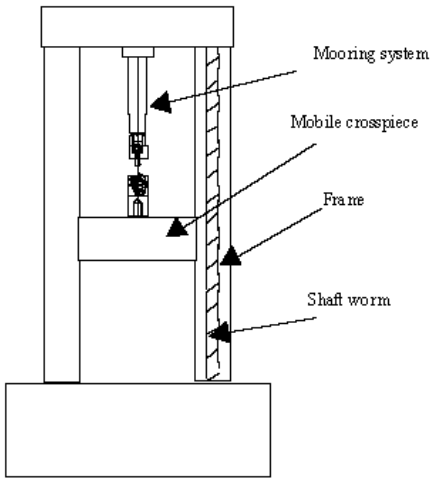

Fig. 8: Diagram of a universal testing machine type Instron 1185

A pressure axis: This axis is designed with concave extremity to fit the external shape of the ball bearing hold by a compensation ring disposed in its core. These components are treated steel made to raise its rigidity.

The control device: The load to be applied, the loading speed as well as the parameters of testing conditions with the system response are all programmed on the control device desk.

Data acquisition: The system response is collected at the plotting table, with deformations in X-coordinate and loads in Y-coordinate. These data are simultaneously transferred and stored in a computer.

EXPERIENCE

Experimental conditions: The stiffness measure of the ball bearing (assembled system rings and balls) requires supported loads. Moreover, the loading speed must be the weakest. In case of these presents test, the load is limited according to SKF reference at 4000 N and the loading speed is taken equal to 0.05 (mm mn^{-1}) (this speed is translated into crosspiece displacement term).

The ball bearing is fit between the pressure axis and compensation ring (Fig. 9), the test is launched at the moment when the contact between all parts is done. The total deformation is then measured on the ball bearing (Fig. 10).

Test

Testing with ball bearing: Figure 11 shows the assembly which allows measure of the whole system stiffness. Two cases are considered. In the first one, the ball is placed in the loading axis. In the 2nd one, the loading axis passes between 2 balls.

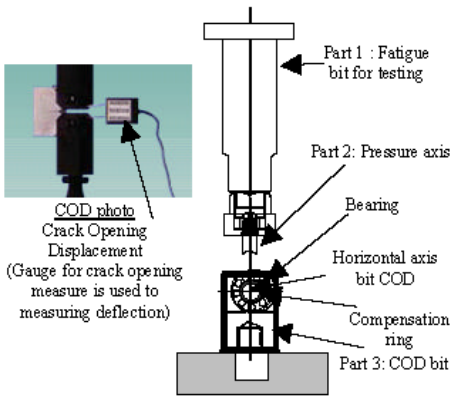

Fig. 9: Ball bearing mooring

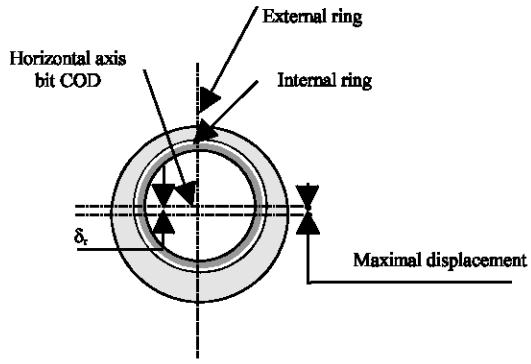

Fig. 10: Ball bearing total deformation

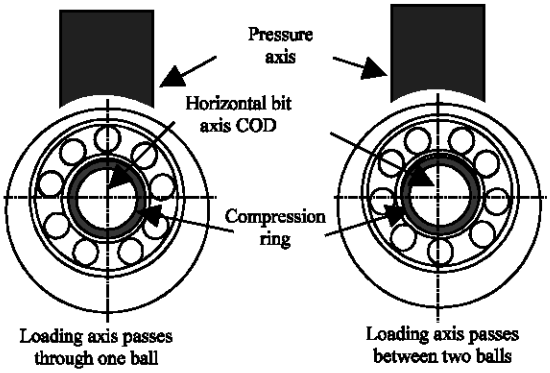

Fig. 11: Loading cases

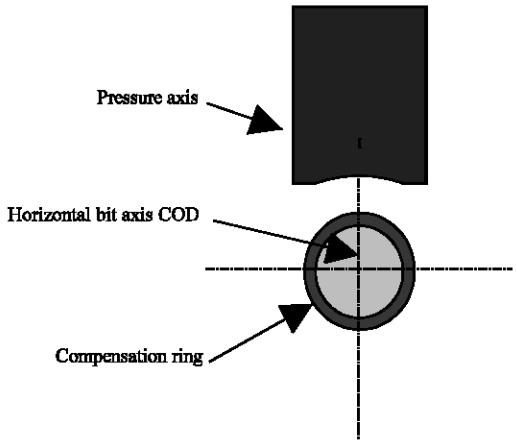

Fig. 12: Testing without rolling

Testing without ball bearing: In this testing the pressure axis directly comes to butt against the compensation ring. This assembly (Fig. 12) allows the system stiffness measure without ball bearing.

RESULTS AND DISCUSSION

The theoretical behaviour model's results of the ball bearing in static mode are shown in Fig. 13a.

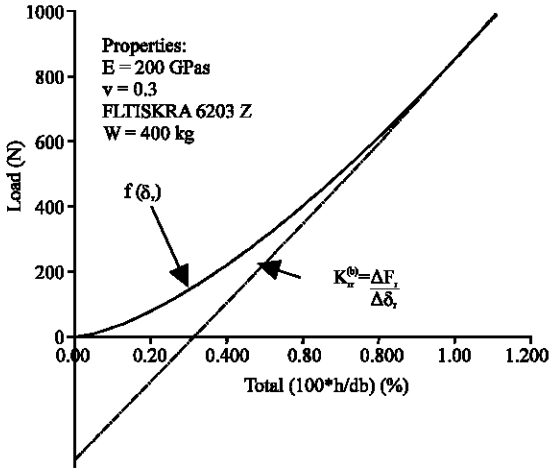

Fig. 13a: Stiffness ball theoretical behaviour (force-displacement) $f(\delta_T)$ curve

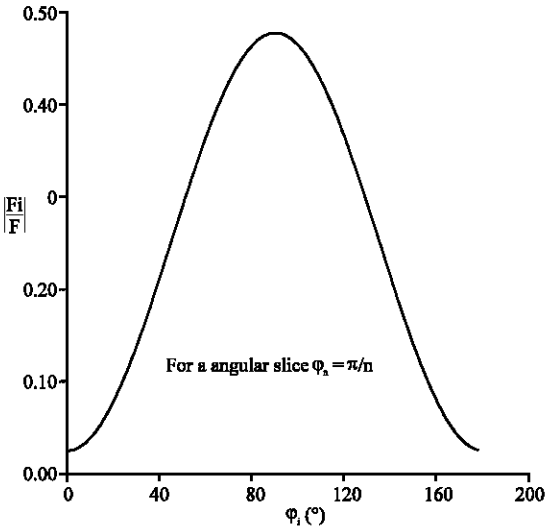

Fig. 13b: Applied force Fi Variation for i^{2nd} ball at position φ_1

Loading distribution on balls is illustrated on Fig. 13b. We note that this loading is not uniform on the balls. Consequently, the ball or the balls being on load axis are the most loaded.

The first 2 figures represent the similar testing results realized on 2 ball bearings (R1 and R2). In these tests, the loading axis passes through one ball (Fig. 14). Figure 15 presents the test where the loading axis passes between 2 balls of the ball bearing (R1).

Figure 16 represents the comparison testing results of the 2 ball bearings. Where, we realize that the ball bearings give too similar curves forms to each other.

In the following, we try to clarify the position change effect of balls according to the loading axis. Figure 17

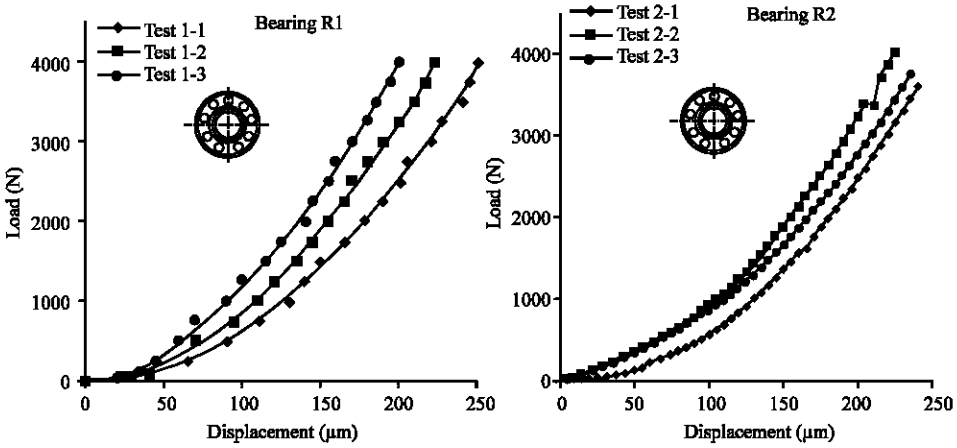

Fig. 14: Testing results with loading axis passes through one ball

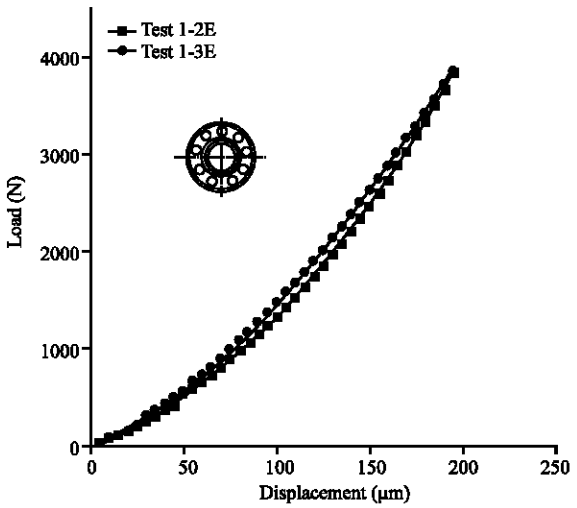

Fig. 15: Testing results of loading axis passes through 2 balls (R1)

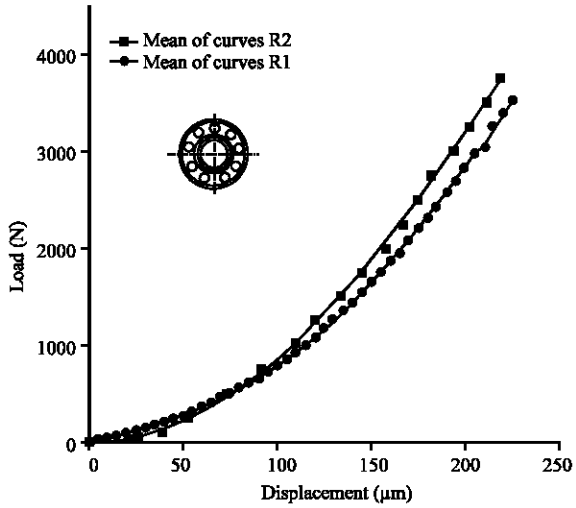

Fig. 16: Comparison testing results from the 2 bearings (case: 1 ball)

shows that if the loading axis passes through one ball the deformations are more important than the case where the loaded axis passes through 2 balls.

The theoretical results represented in Fig. 18 highlight the stiffness variation for 2 ball bearing position configurations. These results are rather similar to those of Fig. 17.

For a detailed comparison, theoretically we change the ball's position angle (φ_i) (Fig. 19 a). Experimentally, we can only take 3 positions at 90° (on the axis) and 90±22.5° (through 2 balls) (where, $\varphi_n = 2\pi/n = 45°$, n = 8) (Fig. 7).

For the theoretical calculation, we use Eq. (7) to obtain the graph of displacement-angle in quasi-static mode.

On the other hand, Fig. 19b represents the graph of the stiffness time variation (i.e., according angles). To obtain this figure, it is sufficient to compute the stiffness according to Eq. (10) by respecting the train (cage) kinematics.

Comparison between the theoretical an experimental displacement-angle curves in the Fig. 19a shows that theoretical curve approaches the experimental one. On the other hand, we can see that displacement-angle curves of Fig. 19a are similar to rigidity-time curve Fig. 19b. Results Fig. 19a in calculated in quasi-static mode can also approach those of dynamic mode.

In conclusion, we can say that experimental and the theoretical verifications of the stiffness model for dynamic conditions gives satisfactory results.

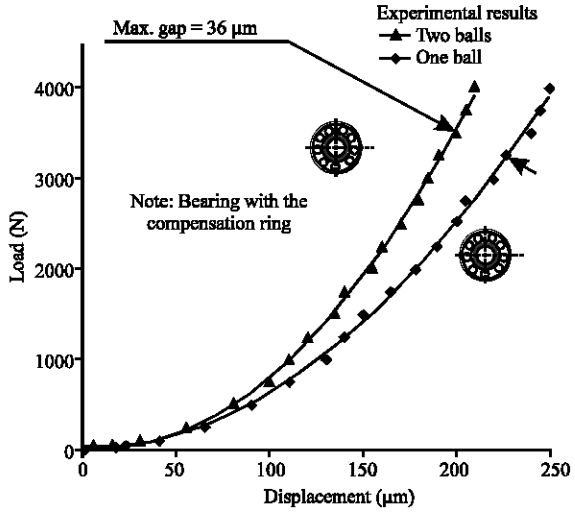

Fig. 17: Testing results of loading axis passes through 1 and 2 balls

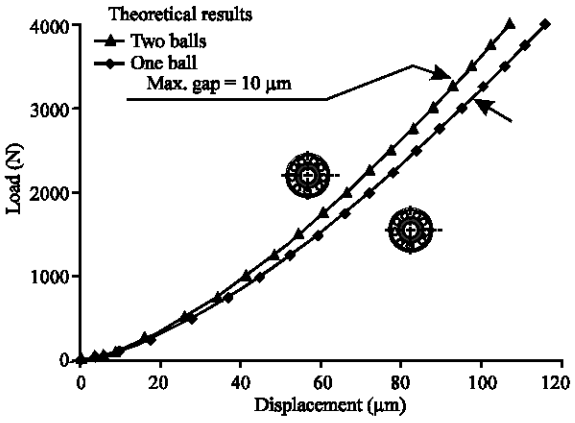

Fig. 18: Theoretical results of loading axis passes through 1 and 2 balls billes

The last experiences, we will show results from which we deduce ball bearings stiffness from holding system (Fig. 20).

The remarks deduced can be enumerated as follows:

- The nonlinearity of the force-displacement curve (Fig. 13) which is similar to that of Lim and Chin (1989), Kraus *et al.* (1987), Lelkes (2002) and the companies Flygt (2004) and Romax (2007)
- The similarity between realized tests under the same conditions
- The ball bearing compensation ring, at the time of test, influences the experimentation by increasing the measured displacement

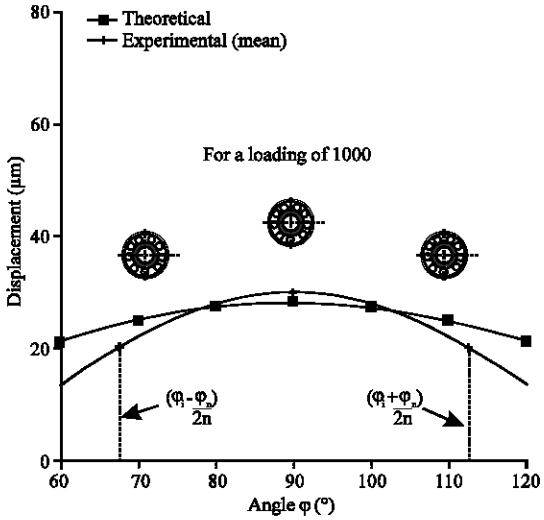

Fig. 19a: Displacement change in function of ball's position angle φ_i (ball scrolling effect for an angular φ_n)

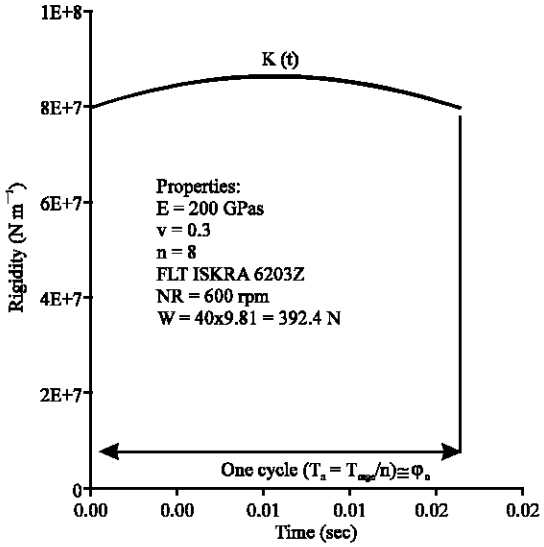

Fig. 19b: Dynamic bearing stiffness K(t) for an angular φ_n (rigidity time)

- A difference exists between tests with ball on axis and ball outside axis. This difference lets believe that the ball bearing stiffness changes according to the balls positioning in the cage (the balls scrolling effect)
- The change from one specimen (ball bearing) to another makes no palpable variation in system response. This results reproduction translates the ball bearings production fidelity. We must note that ball bearings used have the same reference and the same trademark

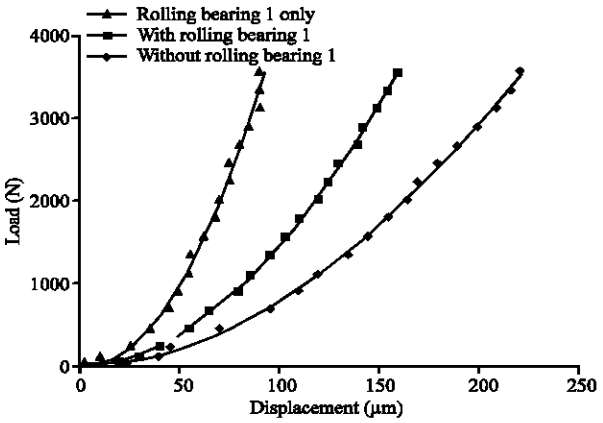

Fig. 20: Deduction of the ball bearing deformation

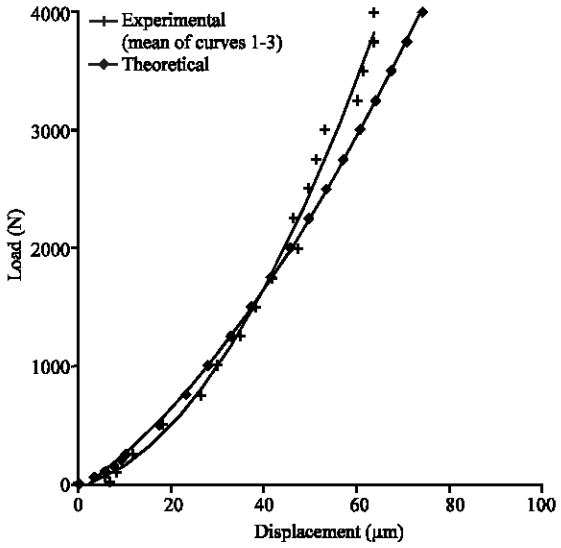

Fig. 21: Comparison of the theoretical and experimental curves

Comparison between the experimental results and those drawn from the theoretical model reveals the following Fig. 21.

Globally, the curves forms result from the modelling reflects the experience relatively.

- At experimental curves beginning a gap exists; this is explained by a small adaptation cycle of crossing system where the functional gaps are caught
- A similarity between experimental results curves into the ball bearing working range
- A relative divergence of values at extreme loads. This stiffness difference can be explained by non consideration of developed model neither to material thermal treatments nor to material face treatments of the ball bearing undergone in reality

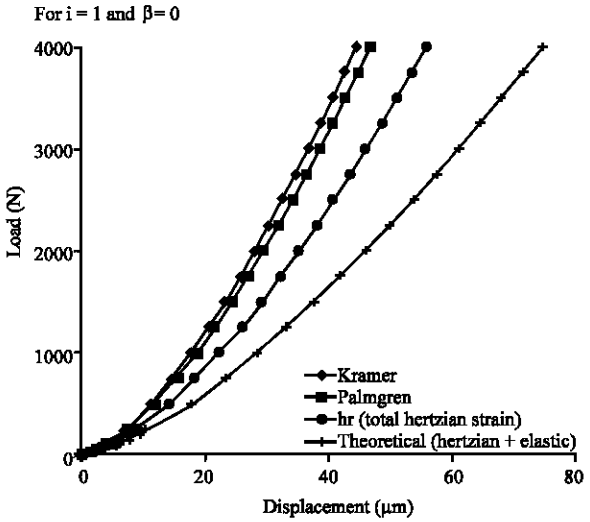

Fig. 22: Superposition of our theoretical model to Palmgren (1967) and Krämer (1993)

In the Fig. 22, we are going to compare our model results to those found in literature. We make hints to Krämer and Palmgren models. We use Eq. (11 and 12) to trace the curves.

Comparison of our results to those of Palmgren (1967) and Krämer (1993) shows that the local deformation curve h_r is proximate to those of Palmgren and Krämer. For the total deformation curve, when we have considered a different approach to compute deformations, presents a perceptible difference; though the comparison of our results to experimental shows a good similarity.

CONCLUSION

The experimental study gives results considered satisfactory. Allowing with a relative tolerance to check the developed theoretical model of the ball bearing stiffness.

This has also allowed experimental measure concretization of ball bearing stiffness and let show through experimentation the difficulties related to mechanical testing devices.

It is concluded that modelling relatively reflects experience, particularly in the ball bearing working range.

On the other hand, experimental curve of the displacement-angle was similar to theoretical curve. This can be used to approach the dynamic stiffness.

Moreover, in static mode the comparison of our model, checked experimentally, to the existing ones shows acceptable similarity with local deformation and perceptible difference with total one, this can be explained by some theoretical different considerations.

REFERENCES

Beatty, R.F. and B.F. Rowan, 1982. Determination of Ball Bearing Dynamic Stiffness, Rockwell International Canoga Park CA Rocketdyne Div.

Bogard, F., K. Debray and Y.Q. Guo, 2002. Determination of sensor positions for predictive maintenance of revolving machines. Int. J. Solids Struct., 39: 3159-3173.

Bourdon and Adelin, 1997. Modélisation dynamique globale des boites de vitesses automobiles, thèse doctorat à INSA de Lyon, ISAL0084, No. 97, pp: 23-42.

Bourgain, L., R. Dart and J. Bourgain, 1988. Machines tournantes et circuits pulsés. Applications Industrielles et médicales de l'analyse spectrale, Dunod, Edition Bordas, pp: 392-411

Campedelli, J., 2002. Modélisation Globale Statique Des Systèmes Mécaniques Hyperstatiques Pre-chargés. Application a un Bogie Moteur, Thèse de Doctorat à L'insa De Lyon, Isal 0102, No. 02, pp: 25-28.

Chevalier, 1979. Guide du dessinateur industriel. Classique Hachette. Edition, pp: 188-189.

De Mul, J.M., J.M. Vree and D.A. Maas, 1989a. Equilibrium and associated load distribution in ball and roller bearings loaded in 5° of freedom while neglecting friction. Part I: General theory and application to ball bearings. Trans. A.S.M.E. J. Tribol., 111: 149-155.

Dehez, B., 2004. Elaboration et application d'une approche multidisciplinaire pour la conception d'un actionneur électrique à rotor sphérique, Thèse de doctorat soutenue à Université catholique de Louvain en, pp: 295-30.

Eschmann, P., L. Hasbargen and K. Weigand, 1985. Ball and Roller Bearings. Theory, Design and Application, R, Oldenburg Verlag, John Wiley and Sons, Inc.

Estocq, P., 2004. Une Approche Méthodologique Numérique et Expérimentale D'aide à La Détection et au Suivi Vibratoire de Défauts D'écaillage de Roulements À Billes, Thèse De Doctorat, Université De Reims Champagne Ardenne, pp: 35-51.

Flygt, I.T.T., 2004. Industries, Engineering for life. Shaft and Bearings Calculations. N°: 02.03. Eng. 0,5 M. 04.04 892932, pp: 7. www.flygt.com.

Fukata, S., E.H. Kondou, T. Ayabe and H. Tamura, 1985. On the Radial Vibration of Ball Bearing. Bull. JSME., 28 (239): 899-904.

Harris, T.A., 1966. Rolling Bearing Analysis. 3rd Edn. Lavoisier, 1991.

Hentati, T. and Col, 2005. A finite element development for ball bearing nonlinear stiffness modelization. Int. J. Simul. Model, 3: 118-128.

Krämer, E., 1993. Dynamics of Rotors and foundation. Berlin, Springer-Verlag.

Kraus, J., J.J. Blech and S.G. Braun, 1987. *In situ* determination of roller bearing stiffness and damping by modal analysis. Trans. A.S.M.E. J. Vibrat. Acoustics Stress and Reliab. Design, 109: 235-240.

Lelkes, M., 2002. Définition des engrenages klingelnberg, Thèse de doctorat présentée à l'INSA LYON, N° d'ordre 02-ISAL-0012, année, pp: 106-110, 125-127.

Lim and T. Chin, 1989. Vibration transmission through rolling element bearings in geared rotor systems. The Ohio State University, pp: 12-60.

Louf, F., 2003. Contact: Théorie De Hertz. Année, pp: 1-7. http://agregb1.Dgm.enscachan.fr/documents/theorietp/files/contact.pdf.

Marsh, R. and D.S. Yantek, 1997. Experimental measurement of precision bearing dynamic stiffness. J. Sound Vibrat., 202 (1): 55-66.

Moret, M., 1995. Roulements et butés à billes et à rouleaux, Techniques de l'ingénieur, Vol. B5-I, Août.

Palmgren, A., 1959. Ball and Roller Bearing Engineering. 3rd Edn. S. Burkank and Co, Philadelphia.

Palmgren, A., 1967. Les roulements, description, théorie, applications, SKF PARIS, pp: 120.

Rajab, M.D., 1982. Modelling of the transmissibility through rolling-element bearing under radial and moment loads. Ph.D. Thesis. The Ohio state university. Columbus. Ohio.

Romax, 2007. Technology-Technical support, Tools for Engineering Excellence, Bearings Questions and Answers Guid. http://www.romaxtech.com/index.php.

Shigley, J.E. and L.D. Mitchel, 1983. Mechanical Engineering Design. 4th Edn. McGraw-Hill, pp: 85-88, 484-514.

Timoshenko, S., 1968. Résistance des matériaux. Théorie élémentaire et problèmes, année, tome I, collection Dunod technique, pp: 2-19.

Yakhou, K., 1999. Validation expérimentale d'un modèle dynamique global de boite de vitesses automobile, Thèse de doctorat, laboratoire de conception et analyse des sciences mécaniques de l'INSA de Lyon, pp: 31-34.

Young, W.B., 1988. Dynamic Modelling and Experimental Measurement of Gear Shaft and Housing System, M.s. Thesis, the Ohio State University, Columbus, Ohio.

Yuzhong, C., 2006. Modelling of high-speed machine-tool spindle systems. Thesis for Doctor of Philosophy in the Faculty of Graduate Studies, the University of British Columbia, pp: 20-82.